EQUIVALENT CIRCUIT MODELING OF WOOD AT 12% MOISTURE CONTENT

Samuel L. Zelinka†

Materials Engineer
USDA Forest Products Laboratory
One Gifford Pinchot Drive
Madison, WI 53726

Donald S. Stone

Associate Professor
College of Engineering
University of Wisconsin
Madison, WI 53706

and

Douglas R. Rammer

Research General Engineer
USDA Forest Products Laboratory
One Gifford Pinchot Drive
Madison, WI 53726

(Received April 2007)

ABSTRACT

Electrical impedance spectra (EIS) were collected from southern pine (*Pinus spp.*) wood equilibrated to 12% moisture content. Cylindrical graphite electrodes were embedded in the wood so that they met nearly end-to-end along a line parallel to the grain, and the EIS properties were characterized as functions of electrode spacing and electrode contact pressure at frequencies between 1×10^{-1} and 3×10^{5} Hz. The data show a narrow distribution of relaxation times, which can be fit using a Debye model or, even better, a model with a constant phase element (CPE) in parallel with a resistor. The relaxation time is sensitive to contact pressure applied to the electrodes but not electrode spacing. The width of the CPE distribution is sensitive to electrode spacing but not contact pressure. On first inspection, the data suggest a finite contact resistance between wood and electrode, but further examination reveals that the "contact resistance" is an artifact caused by electrode fringe effects.

Keywords: Electrochemical Impedance Spectroscopy (EIS), electrical relaxation, contact resistance, corrosion test methods.

INTRODUCTION

Electrochemical test methods show great promise in their ability to rapidly evaluate the corrosion rate of metals in contact with wood (Zelinka and Rammer 2005a, 2005b). Electrochemical tests have numerous advantages over metallic weight loss methods including the ability to be conducted *in situ* at any temperature or wood moisture content. Weight loss methods, on the other hand, tend to be restricted to conditions of rapid corrosion where measurable effects accumulate in a relatively short time.

Among electrochemical test methods, electrochemical impedance spectroscopy (EIS) appears especially promising because it allows the scientist to model the corrosion reaction with an equivalent circuit model. This model, once it has been fit to the data, is then used as a basis for extrapolating data to conditions of interest (Mac-

† Member of SWST

Donald and Johnson 1987). An equivalent circuit model treats the material system as a collection of electrical components such as resistors and capacitors placed in series or parallel so that the collection replicates the frequency response of the real system. A key to the equivalent circuit model is that behaviors represented by components in the model can be understood in terms of physical mechanisms. Both Jack and Smedley (1987) and Zelinka and Rammer (2005b) have published EIS data on wood. Although the former authors analyzed their data using an equivalent circuit model, they did not go so far as to offer a physical interpretation.

A physical interpretation of EIS corrosion data in wood has not been developed because of the complexities of electrical transport in wood. While EIS data collected from experiments in wood give information about corrosion reaction on the surface of metal, this information is convoluted with information about electrical and ionic transport through wood to other electrode(s). The EIS data are further complicated by the wood–electrode interface. The solid-solid interface between electrodes and wood may give rise to additional interfacial polarization, which, if present, needs to be accounted for in the equivalent circuit model (James 1975). Before EIS corrosion data can be interpreted, a better understanding of the electrical properties of wood and wood metal interfaces is needed.

The purpose of the present article is to present preliminary EIS data in a larger, systematic exploration of the electrical properties of southern pine (*Pinus spp.*) so that EIS can become a viable corrosion test method. Whereas many works on the electrical properties of wood have been published previously, very few of these have used impedance spectroscopy. A major difference between impedance spectroscopy and other electrical measurements is that a single impedance spectrum involves many impedance measurements over a large range of frequencies, whereas most published data on the electrical properties of wood pertain to only one frequency or several discrete frequencies. To create an equivalent circuit model, which is necessary for future corrosion tests, it is necessary to know how impedance changes with frequency; this requires the use of impedance spectroscopy or a similar method.

Several papers have shown that electrical measurements in wood are highly dependent on electrode configuration and contact pressure. Vermaas (1975) classified the effect of contact resistance by using electrodes made of different materials. He ran identical tests using electrodes made of nickel-plated brass and a conductive rubber, with the hypothesis that the more compliant rubber would be able to make better contact to the wood surface. In addition, Vermaas took resistance measurements at several pressures with both materials. Vermaas found that measured resistance was always lower when measured with rubber electrodes. He also found that measured resistance decreased with increasing pressure regardless of electrode material. Stamm (1964) reports that contact resistance can be eliminated only when pressure is high enough to cause plastic deformation in wood or electrodes. Stamm found the lowest contact resistance by placing pools of mercury on wood and running current through those pools. James (1985) has shown that applied compressive stress along the grain of wood increases measured conductivity. Neither paper mentions whether change in measured electrical properties with pressure was due to a change in contact resistance or to a change in the actual electrical properties of wood.

These papers highlight complications that arise when trying to measure electrical properties of wood. Directly applying data from the literature as a correction factor to the previous corrosion test of Zelinka and Rammer (2005b) could lead to incorrect conclusions. By using EIS to create an equivalent circuit model, we may be able to separate out changes in bulk properties from changes at the interface. This knowledge can possibly be used to design an optimal electrode configuration and pressure.

The primary objective of this series of measurements was to develop an equivalent circuit model of electrical properties of wood at 12% moisture content, which can be used as a starting point for modeling the corrosion reaction in

wood. Furthermore, this experiment was intended to clarify the role of the wood–metal interface in electrical measurements by observing how parameters in the model change with pressure and electrode spacing. It was believed that this understanding of the wood–metal interface could suggest an optimal electrode configuration for electrochemical corrosion measurements in wood.

EXPERIMENTAL WORK

The experiments were carried out in a manner similar to previous EIS corrosion measurements conducted in wood (Zelinka and Rammer 2005b). A schematic of the test setup is shown in Fig. 1. Since the major objective of the current study was to measure baseline impedance spectra of wood when there is no corrosion occurring, graphite was used for both the working and counter electrodes. Also, since the same material was being used for both the working and counter electrodes, a reference electrode was not necessary (Mansfeld 2003). The lead for the reference electrode was attached to the counter electrode, which resulted in all measurements being taken at zero volts with respect to open-circuit potential. Measurements were made with a Gamry® PCI4-300 potentiostat (Gamry Instruments, Warminster, Pennsylvania). Root mean square amplitude of applied voltage was 10 mV, and the range of frequencies tested was 3×10^{5}Hz to 1×10^{-1}Hz.

The working and counter electrodes were made from a graphite rod with a diameter of 12.7 mm (0.5 in.); the ends were exposed to give a planar interface. The remainder of graphite rods was covered in polytetrafluoroethylene (PTFE) tape, which was held in place by polymeric heat-shrink tubing. These electrodes were placed into predrilled holes in the wood.

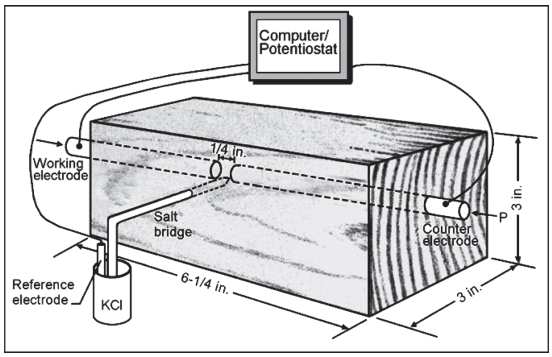

FIG. 1. Corrosion test of Zelinka and Rammer (2005b).

Measurements were made on a "cell" constructed from a piece of straight-grained southern pine (*Pinus spp*.) nominally 102 mm by 102 mm (4 in. by 4 in.). This wood was conditioned and the tests were run in an environmental chamber at 23°C (74°F) and 65% relative humidity. According to the *Wood Handbook,* these conditions should correspond with a moisture content of roughly 12% in southern pine (Forest Products Laboratory 1999). The moisture content, measured gravimetrically, was later found to be between 11.6% and 12.1%. While the original corrosion experiments were run in a 159-mm- (6.25 in.-) long-cell (Zelinka and Rammer 2005b) to reduce the influence of wood drying in the test area, the current experiment ran tests on blocks of wood that were only 50 mm (2 in.) long because tests were run in the same room where the samples were conditioned.

Electrode spacing and contact pressure were two quantities that varied independently in this study, and their effects on the equivalent circuit model were studied. Since preliminary data (Zelinka and Rammer 2005b) contained several distinct relaxation times, the authors believed that one of these relaxation times might represent partial charge transfer at the interface because solid electrodes are in imperfect physical contact with a solid material. The authors hypothesized that an increase in pressure would force these electrodes into better contact and minimize the effect of the wood–metal interface. However, because it is unclear from the literature whether increasing contact pressure of the electrodes affects bulk electrical properties of wood, measurements were taken over various electrode spacings at all pressures. By taking measurements at several distances, a resistance vs. distance curve can be generated. Extrapolating this curve to zero electrode spacing gives contact resistance. It would then be possible to

compare how this extrapolated contact resistance changes with pressure.

Five specimens were machined from wood blocks, each specimen with a different electrode spacing (3.18, 6.35, 12.7, 19.0, and 25.4 mm). Nine pressures were applied to each of the five specimens (1.55, 3.10, 4.65, 6.21, 7.75, 9.31, 10.9, 12.4, and 14.0 MPa). The 14.0-MPa pressure could not be applied to the specimen with the 3.18-mm electrode spacing without causing the graphite electrodes to buckle; so data were not collected for this combination of pressure and spacing.

Pressure was applied by compressing the graphite rods together using two plates pulled together by three threaded metal rods. Metal rods were equipped with strain gages, readings from which were used to determine forces in the rods and therefore pressure on the graphite electrodes. Measurements began with the lowest pressure and were taken as pressure was increased. Preliminary results showed that measurements taken as pressure is decreased are nearly the same as measurements taken as pressure is increased.

RESULTS

Before reporting on behavior of the complex impedance, Z, it is helpful to demonstrate the connection between these data and earlier electrical properties data on wood reported in the literature. The majority of literature data are based on the complex dielectric constant rather than impedance. In terms of impedance, the dielectric constant is given by

$$\varepsilon = \frac{1}{j\omega C_c Z}. \quad (1)$$

Here, C_c represents capacitance of an empty cell, which depends upon the geometry of the test, ω is angular frequency, and $j = \sqrt{-1}$. Commonly, rather than showing the imaginary part of the impedance, authors report the loss tangent, or tan (δ), defined as

$$\tan(\delta) \equiv \frac{\mathrm{Im}(\varepsilon)}{\mathrm{Re}(\varepsilon)}. \quad (2)$$

James (1975) has measured Re(ε) and (δ) as functions of frequency and moisture content for Douglas-fir. Figures 2 and 3 compare our data (6.35 mm, 3.1 MPa) with those of James. Present data show the same general trend as the James data for a 5.08-mm electrode spacing.

In all, 44 impedance spectra were collected. The usual way to present these data is using a Nyquist format in which $-\mathrm{Im}(Z)$ is plotted against $\mathrm{Re}(Z)$. Frequency, the independent variable, is contained implicitly within the data. A representative family of curves, with an electrode spacing of 6.35 mm is shown in Fig. 4. Lines show data fits from the CPE model discussed below.

Impedance data in Fig. 4 all appear as single arcs on the complex plane, which means that each set of data is governed by a single relaxation mechanism (MacDonald and Johnson 1987). Impedance data such as these can often be fit with a Debye equivalent circuit model, so named because of its formal equivalence to Debye's (1945) model for dielectric relaxation of polar molecules. In the past, James (1975) used Debye model to fit dielectric data from wood.

A schematic diagram of the Debye model is shown in Fig. 5a. Here, R_1 and R_2 are resistances, and C is a capacitance. From impedances of these elements listed in Table 1, frequency-dependent impedance of the Debye model can

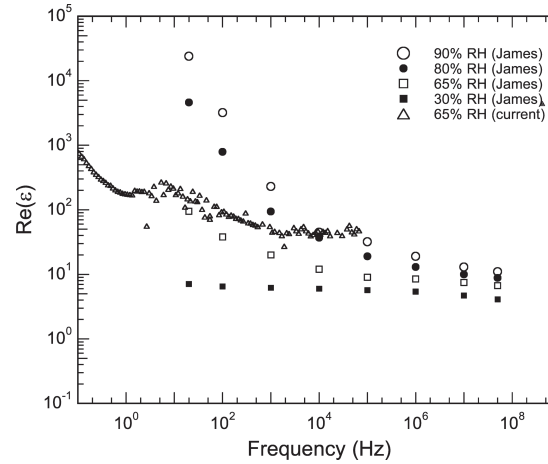

FIG. 2. Current data plotted along with that of James (1975): Re(ε)

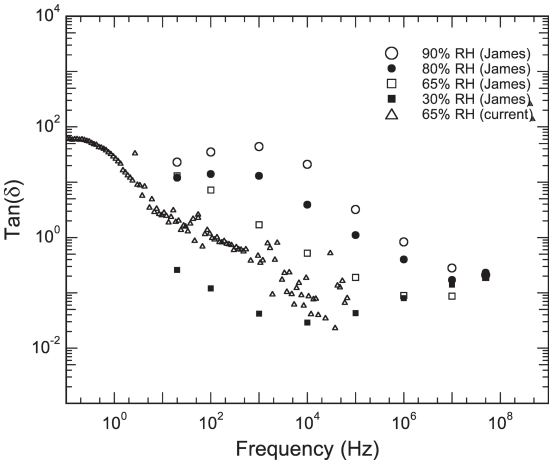

FIG. 3. Current data plotted along with that of James (1975): tan(δ)

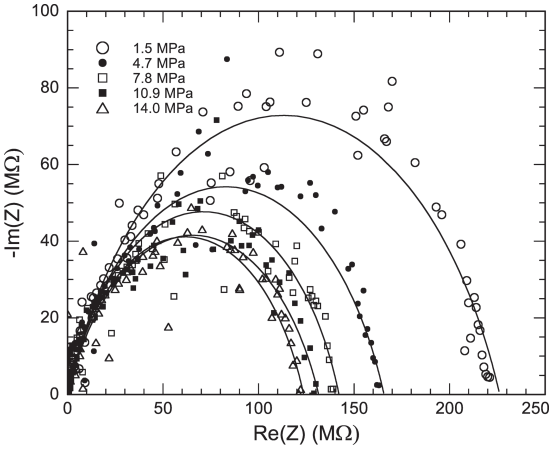

FIG. 4. Representative family of impedance spectra (6.35 mm) represented in the complex plane. The data points represent collected data, and the solid lines represent the predicted behavior from the CPE model (Fig. 5b).

be calculated from elementary circuit theory. This latter impedance is shown in Table 2. Key features of the Debye model are the transition of resistance from $R_1 + R_2$ at low frequencies to R_1 at high frequencies, and a single, characteristic relaxation time, τ_D, equal to R_2C. The approximate frequency at which transition takes place is $\omega \approx 1/\tau_D$. Figure 6 plots real and imaginary components of typical impedance data (3.18 mm and 12.4 MPa) as functions of frequency. A fit of the Debye model generated by using a nonlinear

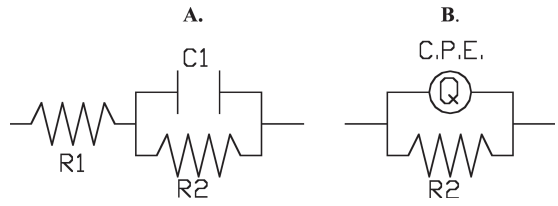

FIG. 5. Schematic diagram of Debye model (a) and 2-element CPE model (b)

TABLE 1. *Impedance expressions for simple circuit elements.*

Element	Impedance expression
Resistor, R	R
Capacitor, C	$\frac{1}{j\omega C}$
Constant Phase Element (CPE), Y_o, n	$\frac{1}{Y_o(j\omega)^n}$

least squares method is also shown in Fig. 6. The Debye model describes data; however, it predicts a sharper transition than is observed. This kind of discrepancy is often seen in the literature and is usually attributed to a distribution of relaxation times rather than the single, well-defined relaxation time assumed by the Debye model. To take into account distribution of relaxation times, the capacitor can be replaced with a constant phase element. Before we go on to the constant phase element, however, it is useful to examine trends of experimental data using the Debye model because the significance of parameters in this model is easily understood.

In fitting the Debye model to experimental data, it was found that R_1 was always several orders of magnitude smaller than R_2. Moreover, R_1 never exhibited any significant trend with either pressure or electrode spacing, and the χ^2-value was relatively unaffected by removal of this parameter. For these reasons, the R_1 parameter was dropped from analysis.

In the absence of R_1, DC resistance of the specimen is determined by R_2. A number of authors have measured DC resistance (Vermaas 1975; Skaar 1964; Simons et al. 1998; Okoh 1977; Langwig and Meyer 1973) using other methods and have sometimes reported that DC

TABLE 2. *Impedance expressions for the models discussed in this paper.*

Model	Total impedance (Z)	Real impedance Re(Z)	Im(Z)
Debye	$R_1 + \dfrac{R_2}{1 + j\omega R_2 C}$	$R_1 + \dfrac{R_2}{1 + (\omega C R_2)^2}$	$\dfrac{\omega C (R_2)^2}{1 + (\omega C R_2)^2}$
2-element CPE	$\dfrac{R_2}{1 + R_2\, Y_o (j\omega)^n}$	$R_2 \left(\dfrac{1 + R_2 Y_o \omega^n \cos\left(\dfrac{n\pi}{2}\right)}{1 + (R_2 Y_o \omega^n)^2 + 2 R_2 Y_o \omega^n \cos\left(\dfrac{n\pi}{2}\right)} \right)$	$\dfrac{(R_2)^2 Y_o \omega^n \sin\left(\dfrac{n\pi}{2}\right)}{1 + (R_2 Y_o \omega^n)^2 + 2 R_2 Y_o \omega^n \cos\left(\dfrac{n\pi}{2}\right)}$

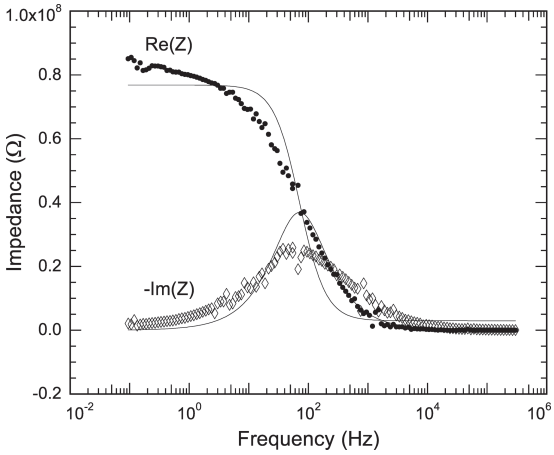

FIG. 6. Real and imaginary components of a typical impedance spectra (3.188 mm and 12.4MPa) as a function of frequency with the Debye model overlay.

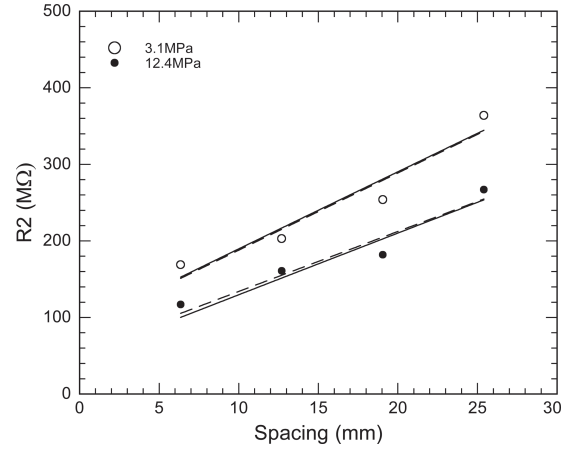

FIG. 7. R2 parameter plotted as a function of electrode spacing with a least squares fit (dashed line) along with a fit accounting for the fringing effects (solid line) for two different contact pressures.

resistance includes an interfacial term. In Fig. 7, we plot R_2 as a function of electrode spacing, and indeed, resistance appears to approach a finite value at zero electrode spacing consistent with the presence of an additional interface resistance. Dashed curves in Fig. 7 are linear least-square fits, which, when they are extrapolated to zero electrode spacing, show the magnitude of the supposed interface resistance. However, a more careful examination of the data reveals that a much more likely explanation for this (apparent) intercept is the fringe effects associated with electric fields between electrodes. This assertion is most readily examined in terms of capacitance, which is plotted against inverse electrode spacing in Fig. 8. According to Slogget et al. (1986), the approximate solution for parallel plate capacitors including fringe effects is

$$C = C_{elem}\left(1 + \frac{2d}{\pi r}\ln\left(\frac{2e\pi r}{d}\right)\right) \qquad (3)$$

where $C_{elem} = \mathrm{Re}(\varepsilon)\varepsilon_0 A/d$ is the value of the capacitance given in elementary treatments. Here, ε_0 is the permittivity of free space, $A = \pi r^2$ the area of the plate, and d the spacing between plates. Curves representing Eq. (3) are superimposed over the experimental data in Fig. 8. Here it is clearly seen that Eq. (3) accounts qualitatively for the trend in C with spacing. Agreement should not be exact because assumptions that enter into Eq. (3), (infinite, isotropic, dielectric, and parallel plate geometry) are not met by the present system. Nevertheless, these disparities seem relatively minor because of the good agreement between results and theory.

Likewise, we can analyze R_2 with a similar

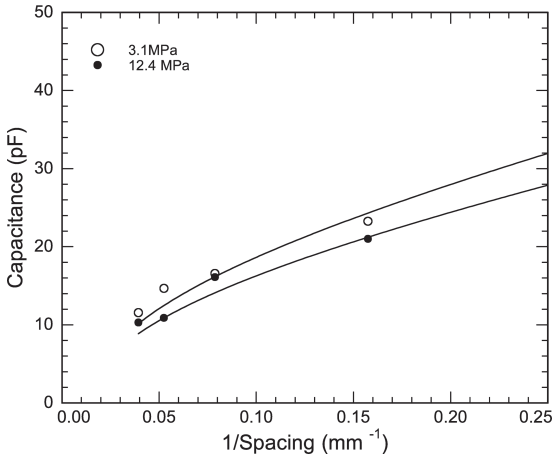

FIG. 8. Capacitance as a function of inverse electrode spacing. The overlay is the predicted value accounting for fringing effects for two different contact pressures.

equation, noting that $1/R_2$ has the same dependence on r and d that capacitance does. Thus, we may write

$$\frac{1}{R_2} = \frac{1}{(R_2)_{elem}}\left(1 + \frac{2d}{\pi r}\ln\left(\frac{2e\pi r}{d}\right)\right) \qquad (4)$$

where $1/(R_2)_{elem} = \omega \mathrm{Im}(\varepsilon)\varepsilon_0 A/d$ is the admittance estimated from an elementary treatment in which current is assumed to flow entirely through the cylindrical region between electrodes. Curves (solid) representing Eq. (4) are superimposed over the data in Fig. 7, where, again, a good agreement is observed. We conclude, therefore, that the apparent intercepts in experimental data, which one might ordinarily take to represent a contact resistance (Vermaas 1975; Skaar 1964), are instead an artifact of electrode configuration.

In AC measurements the frequency at which Re(Z) drops from a high to a low value is given by $\omega = 1/\tau_D$, where τ_D is the relaxation time described earlier. The Debye model predicts this transition to be sharp, that is, to take place within about a decade in frequency. In fact, in Fig. 6, the transition predicted by the Debye model is too sharp and the model is clearly not optimal for the data. This discrepancy is not unique to the data in Fig. 6. All 44 spectra exhibited a slightly broader peak than predicted by the Debye model. Nor is the discrepancy unique to the wood: broadened transitions are widely reported in the literature for non-homogenous materials (Cole and Cole 1941). To handle broadened transitions, constant phase elements (CPE; Fig. 5b, Table 2) are often used. In the CPE model, the parameter n ($0 < n < 1$) is a fitting parameter related to the width of the distribution of relaxation times (Raistrick 1986; MacDonald and Johnson 1987; Cole and Cole 1941). Figure 9 shows the same data as Fig. 6 but fit with the 2-element CPE (Fig. 5b) model instead of the Debye model. As is easily seen, the 2-element CPE model is better able to fit the shape of the more gradual transition than is the Debye model. This improvement is confirmed from a statistics perspective, with a χ^2 value of 6.69×10^{-3} for the CPE model vs. 1.52×10^{-2} for the Debye model. The improved fit allows for a better estimation of parameters.

Because the 2-element CPE model represents a distribution of relaxation times, it replaces the sharply defined relaxation time τ_D of the Debye model with mean relaxation time, τ_o,

$$\tau_o = (R_2 Y_o)^{1/n}. \qquad (5)$$

If we define, then, the parameter $s = 1\mathrm{n}(\tau/\tau_0)$, the distribution in relaxation times, $F(s)$, associ-

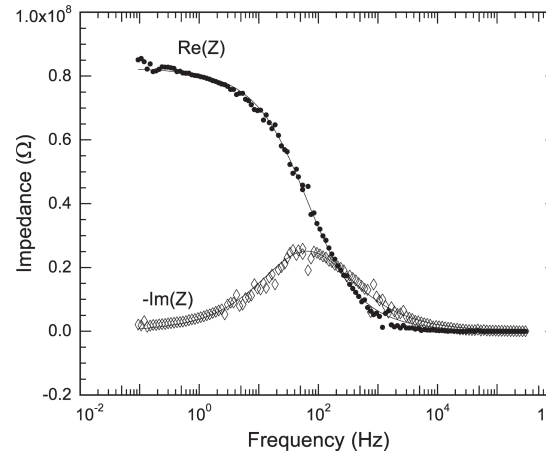

FIG. 9. Real and imaginary components of a typical impedance spectra (3.188 mm and 12.4 MPa) as a function of frequency with the 2-parameter CPE model overlay.

ated by the constant phase element (Cole and Cole 1941; Raistrick et al. 1987) is

$$F(s) = \frac{\sin[(1-n)\pi]}{2\pi\{\cosh(ns\} - \cos[(1-n)\pi]\}} \quad (6)$$

The width, taken as the full width at half of the maximum value (FWHM), of this distribution on a $\log_e$ scale is then

$$w = \frac{2\cosh^{-1}\{2 - \cos[(1-n)\pi]\}}{n}. \quad (7)$$

The mean relaxation time τ_0 is shown as a function of pressure and electrode spacing in Figs. 10 and 11. τ_0 is found to be independent of electrode spacing, a sensible result given that τ_0 is supposed to be a material parameter. Moreover, the independence of τ_0 on electrode spacing is further confirmation that interface resistance and capacitance contribute negligibly to the data because those effects, if present, would be expected to alter calculated values of τ_0 in Eq. (5) depending on how far apart electrodes were spaced. On the other hand, τ_0 clearly depends on pressure in Fig. 10.

The width of distribution, w, is plotted against electrode spacing and pressure a in Figs. 12 and 13. w ranges from about 1.1 to about 2.5, corresponding to factors of 3 to 12 spread in relaxation time. In contrast to the behavior of τ_0, w depends on spacing but not pressure.

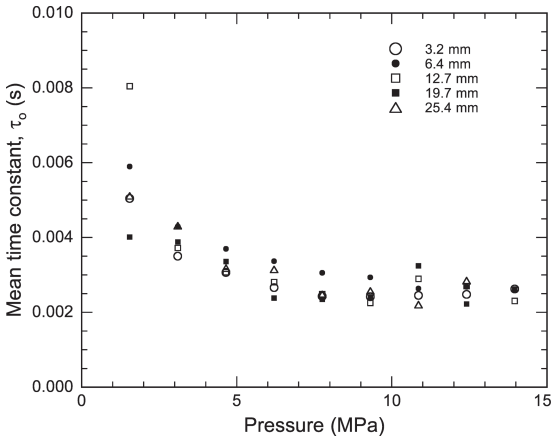

FIG. 10. Mean relaxation time, τ_o, as a function of pressure for various electrode spacings.

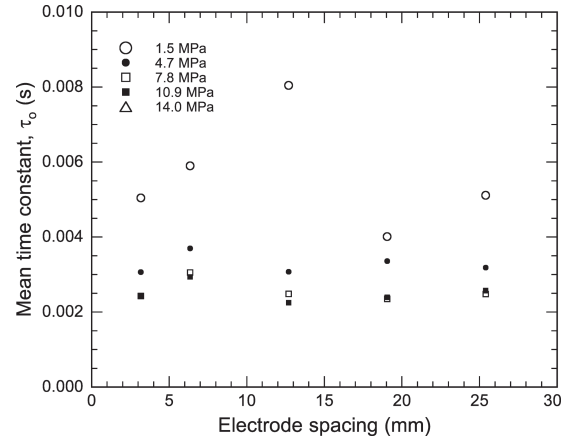

FIG. 11. Mean relaxation time, τ_o, as a function of electrode spacing for various contact pressures.

DISCUSSION

James (1975) has proposed three classes of mechanism to explain the dielectric properties of wood: (a) mechanisms with short relaxation times including electronic, atomic, and fast molecular polarizations; (b) mechanisms with intermediate relaxation times including slow molecular, fixed dipole, and fast interfacial polarizations; and (c) mechanisms with long relaxation times including slow dipole and interfacial polarizations. In James' analysis, most of the frequency dependence of the dielectric constant and tan(δ) in Figs. 2 and 3 comes from slow mechanisms, (c). Given, then, that our data obey a trend similar to James' data, his model could be used to explain the present results; mainly that the observed relaxation most likely arises from a dipole or interfacial interaction.

In this regard, it is interesting that the characteristic relaxation time, τ_0, depends on pressure. Given that the electric properties of wood are strongly influenced by the presence of water (Skaar 1988; Brown et al. 1963; Lin 1965), it is possible that pressure might affect partitioning of water among various chemically or physically distinct sites within cell walls. It is significant that relaxation time, which decreases with increasing pressure, approaches an asymptote at pressures above about 6 MPa, which corresponds to saturation as the sites favored by high

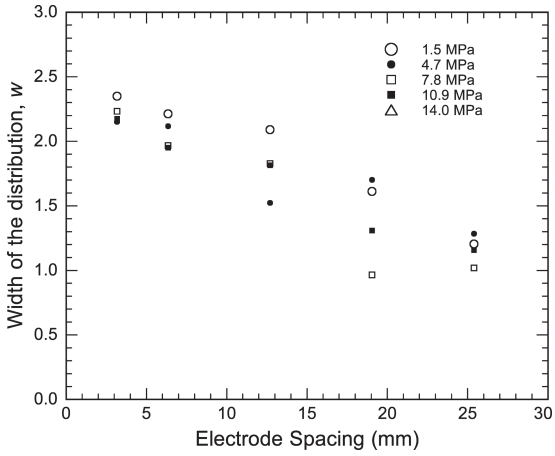

FIG. 12. Width of the distribution, w, as a function of pressure for various electrode spacings.

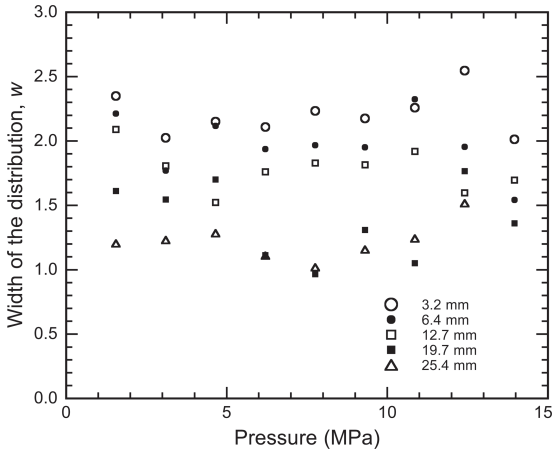

FIG. 13. Width of the distribution, w, as a function of electrode spacing for various contact pressures.

pressure becomes fully populated. An alternative explanation would be that pressure directly influences polarization kinetics. By examining the effects of both pressure and humidity with EIS, it would be possible to observe if change in relaxation time is indeed due to a repartitioning of the location of water within the cell wall.

Width of the distribution, w, is not affected by pressure; instead, it decreases as spacing between electrodes increases, even while τ_0 remains constant. At first glance, it is somewhat puzzling that w decreases with increasing electrode spacing, as we would expect the width of the distribution to increase as more inhomogeneities are incorporated with a larger spacing. However, Y_o, the magnitude the CPE, also decreases with increasing spacing, which we would expect because for a simple capacitor, the capacitance is inversely proportional to spacing. Therefore, we are not comparing equivalent w's when we examine trends of w with electrode spacing because Y_o is changing at the same time, and the size of the distribution depends on the value with it is distributed around.

SUMMARY AND CONCLUSIONS

Electrical properties of southern pine at 12% MC, parallel to the grain, were characterized using electrical impedance spectroscopy. In the range of frequency tested, 1×10^{-1} and 3×10^{5} Hz, data exhibited a single relaxation mechanism, allowing them to be fit with Debye and 2-element CPE models. We concluded that the CPE model fit data better because, in relying on a distribution of relaxation times, it is better able to describe the high-frequency–low-frequency transition in data. Contact resistance effects between wood and electrode were minimal when at least 1.5 MPa of pressure were applied to electrodes. In the CPE model mean relaxation time, τ_0, decreased with increasing pressure but approached a constant value above approximately 6 MPa. Finally, distribution of relaxation times, w, was found to decrease with increasing electrode spacing but to remain constant with increasing pressure.

This research focused on the simple case of electrical contact between wood and metal (graphite) in which there are no added wood preservatives and the electrode does not corrode. Data generated herein can be used as a starting place for understanding and modeling the more complicated situation of corrosion in the presence of wood preservatives, especially when augmented with additional data exploring effects of humidity and pressure. Specifically, the equivalent circuit model for corrosion in wood under these conditions should contain a CPE in parallel with a resistor representing the underlying electrical transport in wood. The spectra

from this experiment, where no corrosion occurred, can be compared with spectra from corrosion experiments, so that the baseline can be removed and only the relevant time constants attributed to corrosion.

By measuring the impedance over a range of frequencies and electrode spacings, we have shown that the contact impedance between wood and electrode were minimal when at least 1.5 MPa of pressure was applied to electrodes. This research has shown that what is sometimes attributed to a contact resistance is most likely due to fringe effects at the electrodes.

It appears that, for all parameters that depend on pressure, they become less sensitive at pressures above 6 MPa. Keeping in mind that these parameters depend on pressure, it appears that consistent readings may be obtained if measurements are made at pressures above 6MPa.

REFERENCES

BROWN, J. H., DAVIDSON, R. W., AND C. SKAAR. 1963. Mechanism of electrical conduction in wood. Forest Prod. J. 13(10):455–459.

COLE, K. S., AND R. H. COLE. 1941. Dispersion and absorption in dielectrics I: Alternating current characteristics. J. Chem. Phys. 9:341–351.

DEBYE, P. 1945. Polar molecules. Dover Publications, New York, NY.

FOREST PRODUCTS LABORATORY. 1999. Wood handbook–wood as an engineering material. Gen. Tech. Rep. FPL-GTR-113 USDA Forest Prod. Lab., Madison, WI.

JACK, E. J., AND S. I. SMEDLEY. 1987. Electrochemical study of the corrosion of metals in contact with preservative treated wood. National Association of Corrosion Engineers. 43(5):251–257.

JAMES, W. L. 1975. Dielectric properties of wood and hardboard: Variation with temperature, frequency, moisture content, and grain orientation. Research Paper FPL 245. USDA Forest Prod. Lab., Madison, WI.

———. 1985. Does mechanical stress affect the dielectric properties of wood? Wood Fiber Sci. 17(3):365–368.

LANGWIG, J. E., AND J. A. MEYER. 1973. Ion migration in wood verified by neutron activation analysis. Wood Sci. 6(1):39–50.

LIN, R. T. 1965. A study of electrical conduction in wood. PhD thesis, State University College of Forestry at Syracuse University, Syracuse, NY.

MACDONALD, J. R., AND W. B. JOHNSON. 1987. Fundamentals of impedance spectroscopy. Pages 1-26 *in* J. R. MacDonald, ed. Impedance spectroscopy emphasizing solid materials and systems. John Wiley & Sons, New York, NY.

MANSFELD, F. 2003. Electrochemical methods of corrosion testing. Pages 446–462 *in* ASM handbook vol. 13A. Corrosion: Fundamentals, testing, and protection. ASM International, Materials Park, OH.

OKOH, I. K. A. 1977. Moisture dependence of DC electrical resistivity of some Ghanaian woods. Technical-Bulletin-of-the-Forest-Products-Research-Institute,-Ghana. 1(2): 33–41.

RAISTRICK, I. D. 1986. Application of impedance spectroscopy to materials science. Ann. Rev. Mater. Sci. 16:343–370.

———, MACDONALD, J. R., AND D. R. FRANCESCHETTI. 1987. The electrical analogs of physical and chemical processes. Pages 27–84 *in* J. R. MacDonald, ed. Impedance spectroscopy emphasizing solid materials and systems. John Wiley & Sons, New York, NY.

SIMONS, P. J., SPIRO, M., AND J. F. LEVY. 1998. Electrical transport of endogenous mineral ions in green sapwood of *Pinus sylvestris L.* (Scots pine). Wood Sci. Technol. 32: 403–410.

SKAAR, C. 1964. Some factors involved in the electrical determination of moisture gradients in wood. Forest Prod. J. 14(6):239–243.

——— 1988. Electrical properties of wood. in C. Skaar. Wood-water relations. Springer-Verlag, Berlin; New York NY.

SLOGGET, G. J., BARTON, N. G., AND S. J. SPENCER. 1986. Fringing fields in disc capacitors. J. Physics A: Mathematical and General 19(14):2725–2736.

STAMM, A. J. 1964. Electrical Properties. Pages 359–385 *in* A. J. Stamm Wood and cellulose science. Ronald Press Company, New York, NY.

VERMAAS, H. F. 1975. Experimental variables affecting the measurement of the DC resistance of wood. Holzforschung 29(4):140–144.

ZELINKA, S. L., AND D. R. RAMMER. 2005a. Review of test methods used to determine the corrosion rate of metals in contact with treated wood. Gen. Tech. Rep. FPL-GTR-156 USDA Forest Prod. Lab., Madison, WI.

———, AND ———. 2005b. The use of electrochemical impedance spectroscopy (EIS) to measure the corrosion of metals in contact with wood. TMS Letters. 2(1):15–16.